

# Directional Channel Characteristics in Elevation and Azimuth at an Urban Macrocell Base Station

Jonas Medbo, Henrik Asplund, Jan-Erik Berg, Niklas Jalden  
Ericsson Research, Ericsson AB, Sweden

**Abstract**—The objective of this paper is to improve the knowledge on directional channel characteristics at the base station, particularly concerning elevation. For this purpose a channel measurement campaign has been performed. A powerful new method for super-resolution channel estimation has been used to get a detailed picture of the directional characteristics of the channel. This has further led to improved knowledge of when processes like diffraction over rooftops and/or specular reflections are important. The findings herein have been incorporated into a model for the elevation angle dispersion which is proposed as an extension to some commonly used directional channel models such as the ITU-IMT-Advanced model.

## I. INTRODUCTION

The directional characteristics of the radio channel are increasingly being utilized for improving the quality and capacity of wireless communication systems, via techniques such as multi-antenna transmission and reception (MIMO), increased directivity (beamforming, sectorization, tilt) etc. Correspondingly, the research efforts on channel characterization have in the past years been focused on measurements and model improvements concerning the directional characteristics of the radio channel. Several directional channel models [1-3] have been developed for use in standardization and development. However, with respect to the elevation characteristics of the radio channel these models are largely insufficient. Little or no measurement support is available, and the common assumption is that the radio waves propagate exclusively in the horizontal plane.

The main purpose of this work is to improve the directional radio channel characterization at the base station (BS) in the urban macro-cell scenario with particular attention paid to elevation. A channel measurement campaign comprising 10 non-line-of-sight (NLOS) outdoor user equipment (UE) locations at distances up to 300 m from the BS location has been performed at 5.25 GHz using 200 MHz bandwidth. Super-resolved channel parameters in direction as well as delay are provided by means of a maximum likelihood based method [4]. Substantial improvements in accuracy and efficiency, relative to standard methods [5,6], have been achieved by modifications with respect to genuine maximum likelihood.

## II. MEASUREMENTS

A schematic drawing of the measurement set-up and a photograph of the scenario are shown in Fig.1. At the BS a directional patch antenna with 7dBi gain ( $90^\circ$  beamwidth) and

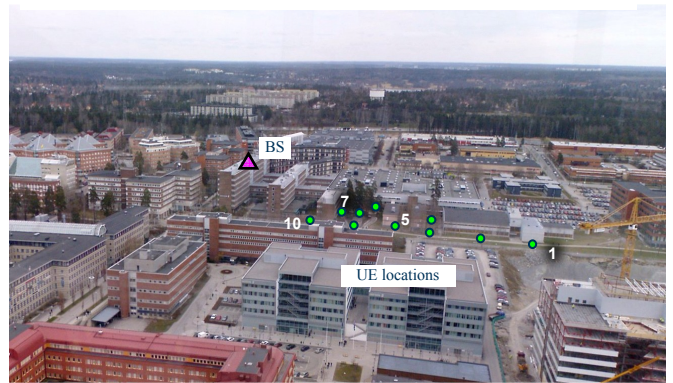
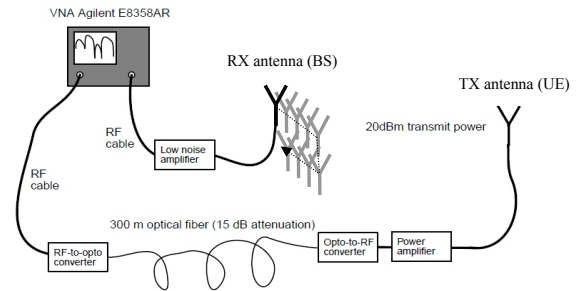


Figure 1. Schematic drawing of the measurement set-up (upper) and photograph of measurement scenario (lower).

vertical polarization was used. A virtual planar array of  $10 \times 25$  elements ( $N_{\text{horizontal}} \times N_{\text{vertical}}$ ), with 2 cm ( $0.35 \lambda$ ) spacing was formed by means of an antenna positioning system based on electro mechanical actuators providing spatial accuracy better than 0.1 mm. In the user equipment (UE) end an ordinary vertical dipole antenna was used.

The channel was measured over 200 MHz bandwidth, using an Agilent E8358A vector network analyzer (VNA). This measurement technique requires that both antennas are connected to the VNA with RF cables. The typical loss for ordinary coaxial measurement cables is at the order of one dB per meter. In order to allow large Tx-Rx antenna separations the RF signal was transmitted over an optical multimode fiber using RF-to-opto and opto-to-RF converters. A laptop was used for control of the antenna actuators and data acquisition.

### III. SUPER RESOLUTION METHOD

The measurement data analysis is based on a novel super-resolved method for estimation of angles and delays. By using a modified likelihood function, by introducing windowing of both the measurement data and the corresponding model, substantial improvement of accuracy as well as computational efficiency has been achieved [4]. The basic principle is to fit a channel model  $\tilde{\mathbf{H}}$  composed of a set of plane waves to the measured channel  $\mathbf{H}$ . The corresponding model is given by

$$\tilde{H}_{mn} = \sum_{l=1}^N \mathbf{g}_m^{\text{rx}}(-\mathbf{k}_l^{\text{rx}})^{\text{T}} \cdot \mathbf{A}_l \cdot \mathbf{g}_n^{\text{tx}}(\mathbf{k}_l^{\text{tx}}) \cdot \exp[j(\mathbf{k}_l^{\text{rx}} \cdot \mathbf{r}_m^{\text{rx}} - \mathbf{k}_l^{\text{tx}} \cdot \mathbf{r}_n^{\text{tx}} + \omega\tau_l)] \quad (1)$$

where  $\tilde{H}_{mn}$  is the channel between tx antenna  $n$  and rx antenna  $m$ ,  $\mathbf{A}_l$  is the complex polarimetric amplitude matrix of the  $l^{\text{th}}$  of totally  $N$  plane waves,  $\mathbf{g}_m^{\text{rx}}(-\mathbf{k}_l^{\text{rx}})$  and  $\mathbf{g}_n^{\text{tx}}(\mathbf{k}_l^{\text{tx}})$  are the complex polarimetric antenna pattern vectors for the corresponding wave vectors  $\mathbf{k}_l^{\text{rx}}$  and  $\mathbf{k}_l^{\text{tx}}$ ,  $\mathbf{r}_m^{\text{rx}}$  and  $\mathbf{r}_n^{\text{tx}}$  are the position vectors of the receive and transmit antenna elements relative to corresponding antenna reference points,  $\omega$  is the angular frequency and  $\tau_l$  is the wave propagation delay between the reference points. The corresponding modified log likelihood is given by

$$-\log L_{\text{mod}} = N_{\text{rx}} N_{\text{tx}} N_f \log(\pi\sigma^2) + \frac{1}{\sigma^2} \sum_{m=1}^{N_{\text{rx}}} \sum_{n=1}^{N_{\text{tx}}} \sum_{k=1}^{N_f} \left\| w_{mnk} \tilde{H}_{mnk} - w_{mnk} H_{mnk} \right\|^2 \quad (2)$$

where  $k$  is the index over frequency samples,  $H_{mnk}$  is the measured channel response,  $w_{mnk}$  is the window function and  $\sigma^2$  is the measurement noise power. The estimation accuracy is given by the method itself in terms of the Fisher information matrix providing the corresponding estimation error for each parameter.

### IV. MEASUREMENT RESULTS

#### A. Measurement Data and Estimation Accuracy

The total measurement time for a single UE location was around 7 minutes since the antenna positioning system took about 1 second for each change of antenna position. Moreover, as it was a bit windy during the measurements the movement of some significant trees affected the measurement data.

At specific delays and directions of arrival and departure the corresponding radio waves are distorted due to time variations created by the moving trees. The result of these time variations is that the power of waves scattered in trees will largely appear as randomly distributed in angle i.e. as noise. The remaining coherent power scattered off the trees is reduced correspondingly meaning that the significance of the trees is underestimated. In order to estimate the power of this noise the fact that each channel sweep in frequency was fast enough (380 ms) to avoid distortions is utilized. The power delay profile corresponding to directions above the skyline is proportional to

the noise power caused by the moving trees. In Fig. 4 the average power delay profiles for wave propagation in directions up towards the sky as well as towards significant scatterers, determined by beamforming, are shown. Since there are no scatterers in the sky the power in this direction corresponds to noise. This noise ranges from 5 to 20 dB below the average power in the directions where the scatterers are located.

For each UE location  $N=500$  waves have been estimated. As described in [4] the estimates are initialized by finding peaks in angle domain above the noise floor. Moreover, the requirement that the standard deviation of the errors of the estimates is less than 40 degrees in angle and 20 meters in propagation distance is set. As shown in Fig. 2 the estimates account for most of the power of the measured channel.

#### B. Angle and Delay Estimation Results

To assure high reliability of the presented results the following analysis is based on paths having estimation errors with standard deviations less than 2 degrees in elevation and 4 degrees in azimuth. The corresponding estimated plane waves superimposed on a panoramic photograph are shown in Fig. 3. It is clear that the dominant paths are diffracted over the roof tops and/or reflected off neighboring buildings. It seems that the main propagation mechanisms are reflections off neighboring buildings which are in LOS condition from both the BS and the UE. At some UE locations (7-10) diffraction

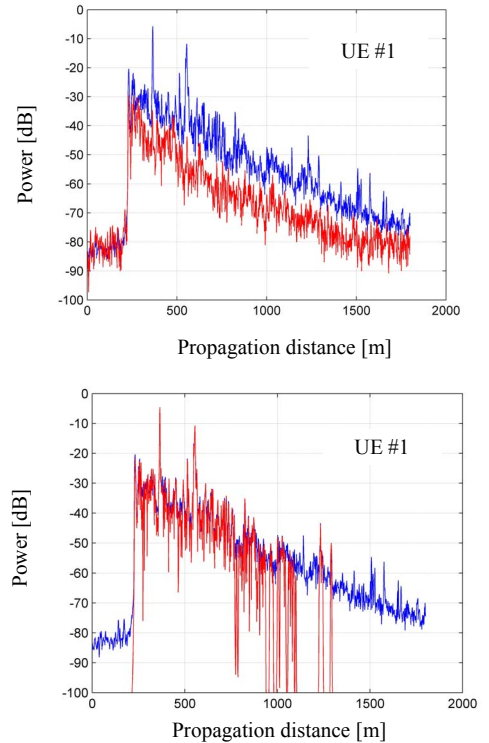


Figure 2. Average power delay profiles corresponding to wave propagation towards significant scatterers (upper blue curves) and in directions above the skyline (red lower line in upper graph), and power corresponding to estimated waves (red line in lower graph) for UE location 1.

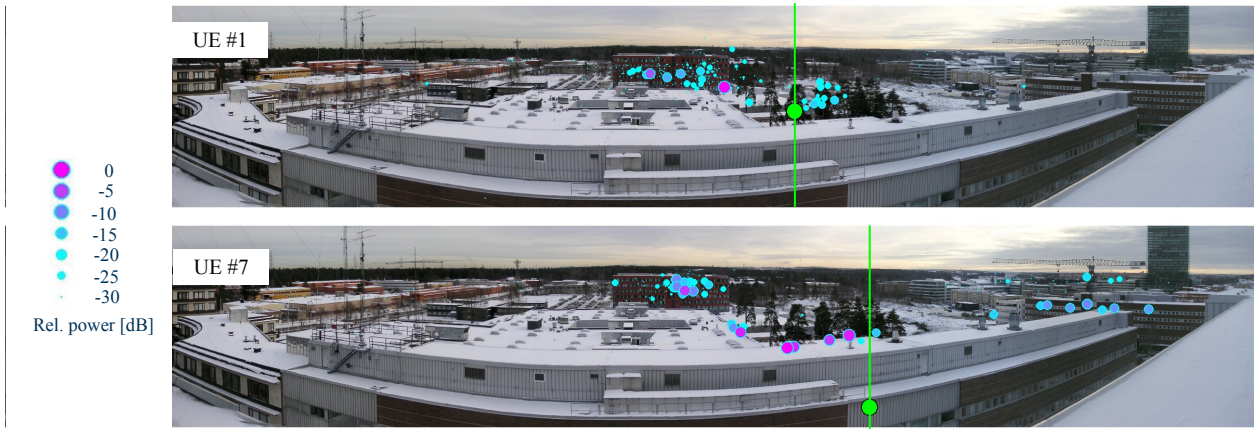


Figure 4. Estimated paths superimposed on a panoramic photograph taken from the BS location at the roof. The directions of the UE locations are indicated with green circles. It should be noted that the UEs are in NLOS conditions so that they are not visible from the BS.

over the rooftops seems to be important.

In order to classify UE locations for which diffraction may be important the excess loss is used. For this particular measurement campaign it seems that the radio link at UE locations for which the excess loss is larger than 25 dB has a significant contribution from diffracted paths. Classification of paths as diffracted or specularly reflected has been done by means of the projected UE location. This is the location obtained by extrapolating the estimated wave direction at the base station to the distance corresponding to the estimated delay. If the projected UE location is on or near ground level, the wave has been classified as specular, whereas if the projected UE location is significantly above ground, e.g. more than half of the height of the closest obstructing building, then the path is classified as diffracted. The corresponding power distributions of elevation angle and path propagation distance for the two sets of UE locations are shown in Fig. 5. It is clear that only for the UEs having excess loss larger than 25 dB there is significant power for projected UE heights larger than 6.5 m. This is also confirmed by comparing the diffracted fraction of total power vs UE locations and excess loss shown in Fig. 4.

In order to get an impression of the overall distribution of

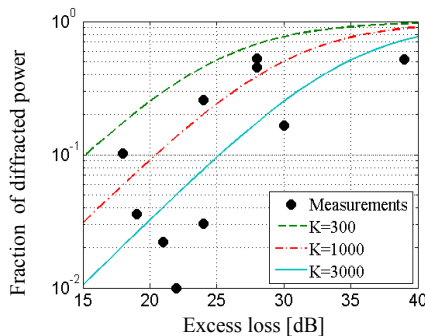


Figure 5. Fraction of total power classified as diffracted versus excess loss (circles). Lines indicate probability of a cluster being diffracted according to the model (6) for three different parameter settings.

angles at the BS aggregate spectra have been determined. For this purpose all estimated paths from all UE locations have been summed using a Gaussian filter for smoothing with standard deviations  $3/\sqrt{2}$  and  $1/\sqrt{2}$  degrees in azimuth and elevation respectively. In Fig. 6 are shown the corresponding spectra for three cases: 1) all paths; 2) paths with projected UE height  $> 6.5$  m; 3) paths with projected UE height  $< 6.5$  m. It is clear that the main scattering objects are the buildings A, B, C

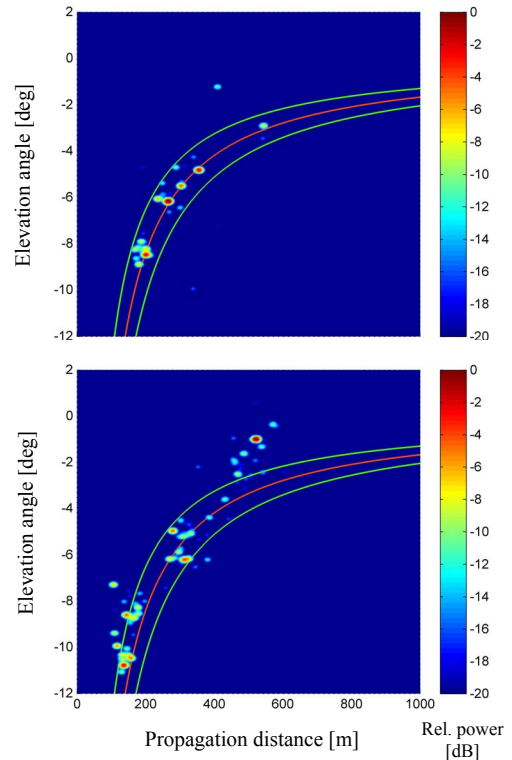


Figure 3. Power distributions in elevation angle and propagation distance for UE locations having excess loss less than 25 dB (upper) and higher than 25 dB (lower). Projected UE heights of -6.5, 0 and 6.5 m above ground are indicated with solid lines.

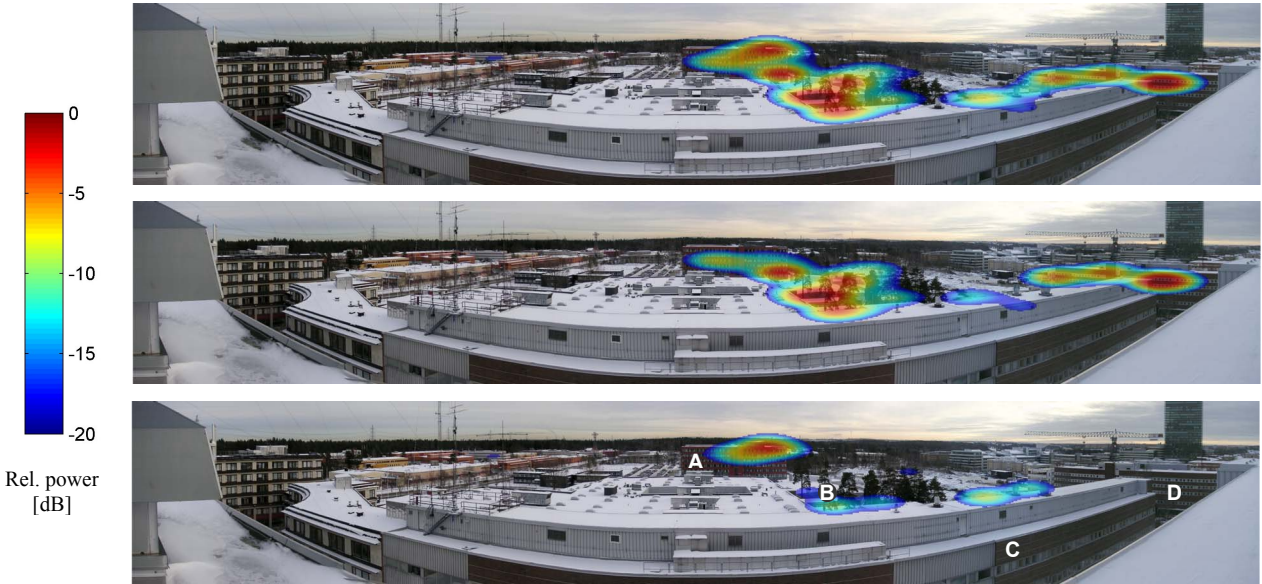


Figure 6. Aggregate directional spectra for all UEs. In the upper graph the distribution for all paths is shown; in the middle graph the distribution for paths with projected UE height  $< 6.5$  m is shown; and in the lower graph the distribution for paths with projected UE height  $> 6.5$  m is shown. The power has been equalized for all UEs.

and D. Moreover, diffraction over the roof top of building C and diffuse scattering at the higher part of building A is important.

### C. Channel Characterization and Wave Estimate Accuracy

In order to assess the impact of wave estimation accuracy on the observed channel characteristics, the analysis has been repeated for different requirements on the wave parameter errors. It is found that the channel characterization sensitivity to wave parameter estimation errors is small for most of the UE locations. This probably a result of that most of the channel power is accounted for by waves having high parameter accuracy. As shown in Fig. 7, more than 80% of the channel power is accounted for using waves with error standard deviations less than 2 degrees in elevation ( $\sigma_\phi < 2^\circ$ ) and 4 degrees in azimuth ( $\sigma_\theta < 4^\circ$ ) except for UE locations 7, 8 and 10. Loosening the accuracy requirements to  $\sigma_\theta < 8^\circ$ ,  $\sigma_\phi < 16^\circ$ , results in that more than 90% of the channel power is accounted for irrespective the UE location. It is also clear that the channel large scale parameters are little affected by using looser error requirements. Consequently those estimated parameters are very reliable. Only for UE location 10 some impact is observed if larger errors of the estimates are allowed. For this UE location one can conclude that the measurement noise power is too high to provide fully accurate channel estimates.

## V. ELEVATION ANGLE MODELING

### A. Desired Model Characteristics

It is desirable to model both specularly reflected paths and over rooftop-diffracted paths as observed in the measurements.

The dependence of the elevation angle on the propagation distance of a path and the correlation between the excess path loss and dominating propagation process should also be captured as shown in Figs. 4 and 5.

The model presented below is intended to be combined with an existing cluster-based spatial channel model such as [1-3].

### B. Model proposal

1. Introduce a clutter height parameter,  $h_{cl}$ , representative of the average building height. This model is applicable to base stations deployed at or above the average roof top height, i.e. for  $h_{cl} \leq h_{bs}$ .

2. For each cluster  $n$ , determine the total path length  $d_n$  from the absolute delay  $\tau_n$  or the excess delay  $\tau'_n$  as

$$d_n = c \cdot \tau_n = d_0 + c \cdot \tau'_n \quad (3)$$

where  $c$  is the speed of light and  $d_0$  is the BS to UE distance.

3. For each cluster, calculate the BS-UE plane elevation angle  $\theta_n^{UEplane}$  and the BS-clutter plane elevation angle  $\theta_n^{clutter}$  as

$$\begin{aligned} \theta_n^{UEplane} &= \arcsin \frac{h_{UE} - h_{BS}}{d_n} \\ \theta_n^{clutter} &= \arcsin \frac{h_{cl} - h_{BS}}{d_n} \end{aligned} \quad (4)$$

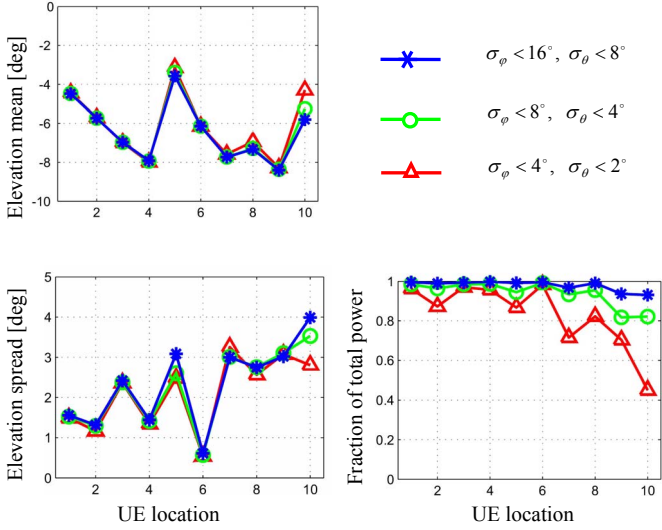


Figure 7. Dependence of channel large scale parameters on accuracy of wave estimates versus UE location. The different curves correspond to different standard deviations of the estimation errors of elevation angle ( $\sigma_\theta$ ).

4. Determine the per-cluster path loss in relation to the free space path loss (in linear scale):

$$s_n = \frac{(\lambda/4\pi d_n)^2}{p_n} \quad (5)$$

where  $p_n$  is the cluster path gain and  $\lambda$  is the wavelength.

5. Determine the per-cluster probability of having the elevation angle  $\theta_n^{clutter}$  (clusters not in the BS-clutter plane will have the elevation angle  $\theta_n^{UEplane}$ ):

$$\Pr \{ \theta_n = \theta_n^{clutter} \} = \frac{s_n}{s_n + K} \quad (6)$$

where  $K$  is a constant that can be used for model tuning, i.e.  $10 \cdot \log_{10} K$  is the excess path loss in dB for which the diffracted power is half of the total power (compare Fig 4).

6. For clusters that are randomly determined to be in the BS-clutter plane, set the elevation angle  $\theta_n$  to  $\theta_n^{clutter}$ , while the elevation angles for the paths in the other clusters are set to  $\theta_n^{UEplane}$ . If a LOS path exists, the elevation angle of this path is set to  $\theta_1^{UEplane}$ .

### C. Example of model realization

Fig. 8 shows one example of a model realization of the SCM model [1] in combination with the proposed elevation model. The parameters used have been  $K=1000$ ,  $h_{cl} = 12$  m,  $h_{BS} = 20$  m,  $d_0 = 150$  m. The distribution of clusters in azimuth, elevation, and delay is in line with the findings of the measurements as is evident from a visual comparison with Figs. 3 and 5.

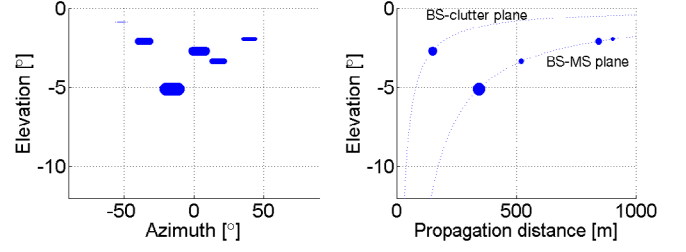


Figure 8. Example of elevation angles and their dependence on azimuth and propagation distance, realized with the proposed model in combination with the SCM Urban Macro model [1]. The area of the circles indicates the cluster power.

## VI. SUMMARY AND DISCUSSION

Highly resolved directional channel information, both in elevation and azimuth, at the base station location has been determined by means of a wideband channel measurement campaign. The measured channel response has been fitted to a model based on plane waves by maximization of the ‘modified’ likelihood. Important insights of main propagation pathways have been gained by the sets of highly resolved paths. The paths are clustered in directions where building walls roof edges or trees have LOS conditions to both the BS and the UE. From the BS perspective there is a limited part of the space angle region which fulfils this LOS condition, forming a mask in azimuth and elevation. It is also clear that the path loss is less when a specular path is possible and larger when diffraction over the roof tops is required. Finally, these findings have successfully been incorporated into a model proposal, intended to conveniently be combined with existing cluster-based spatial channel models.

## REFERENCES

- [1] 3GPP TR 25.996, *Spatial channel model for Multiple Input Multiple Output (MIMO) simulations*, <http://www.3gpp.org/ftp/Specs/html-info/25996.htm>
- [2] P. Heino, ed., “D5.3: WINNER+ Final Channel Models”, [http://projects.celtic-initiative.org/winner+/WINNER+%20Deliverables/D5.3\\_v1.0.pdf](http://projects.celtic-initiative.org/winner+/WINNER+%20Deliverables/D5.3_v1.0.pdf)
- [3] Report ITU-R M.2135-1, *Guidelines for evaluation of radio interface technologies for IMT-Advanced* (12/2009).
- [4] Jonas Medbo, Fredrik Harrysson, “Efficiency and Accuracy Enhanced Super Resolved Channel Estimation,” 6th European Conference on Antennas and Propagation, Prague, Czech Republic, on 26-30 March 2012.
- [5] B. H. Fleury, et al., “Channel Parameter Estimation in Mobile Radio Environments Using the SAGE Algorithm,” *IEEE Journal on Selected Areas in Communications*, Vol. 17, No. 3, pp. 434-450, March 1999.
- [6] Andreas Richter, “Estimation of Radio Channel Parameters: Models and Algorithms,” Doctoral Thesis, ISBN 3-938843-02-0, © Verlag ISLE 2005.